Electronic Supplementary Material (ESI) for Environmental Science: Water Research & Technology.
This journal is © The Royal Society of Chemistry 2020

Electronic Supplementary Information for

Optical Properties and Photochemical Production of Hydroxyl Radical and Singlet Oxygen after Ozonation of Dissolved Organic Matter

Frank Leresche[¤, ⊥], Jeremy A. Torres-Ruiz [†], Tyler Kurtz[⊥], Urs von Gunten[#,‡], and Fernando L. Rosario-Ortiz [¤,⊥, *]

[⊥]Environmental Engineering Program, University of Colorado Boulder, Colorado 80309, United States

[¤] Department of Civil, Environmental and Architectural Engineering, University of Colorado Boulder, Colorado 80309, United States

[†]Department of Chemistry, University of Puerto Rico, Mayagüez, Puerto Rico 00682, United States

[#] Eawag, Swiss Federal Institute of Aquatic Science and Technology, Überlandstrasse 133, CH-8600 Dübendorf, Switzerland

[‡]School of Architecture, Civil and Environmental Engineering (ENAC), Ecole Polytechnique Fédérale de Lausanne (EPFL), CH-1015 Lausanne, Switzerland

[*] Corresponding author: Fernando.rosario@colorado.edu

Number of pages:	18
Number of text sections:	4
Number of figures:	8
Number of tables:	3

Text S1. Chemicals used in the experiments

Pyridine, CAS N_0: 110-86-1, Mallinckrodt chemicals, purity min. 99%. *p*-Nitroanisol, 100-17-4, recrystallized. Furfuryl alcohol, 98-00-0, TCI, 97%. Benzoic acid, 65-85-0, Alpha Aesar, recrystallized. Salicylic acid, 69-72-7, EMD chemicals, 99%. Phosphoric acid, 7664-38-2, EMD Millipore, 85% w/w in H_2O. H_2PO_4Na, 7558-80-7, Alfa Aesar, 96%. $Na_2HPO_4•2H_2O$, 10028-24-7, Fisher Scientific, 95%. *t*-butanol, 75-65-0, Sigma-Aldrich, 99.5%. Acetonitrile, VWR, HPLC grade. Methanol, VWR, HPLC grade.

Text S2. Determination of the photon fluence (E_p^0), the hydroxyl radical ($^{\bullet}$OH) production rate ($r_{\bullet OH}$) and the $^{\bullet}$OH quantum yield ($\Phi_{\bullet OH}$)

The photon fluence, E_p^0 (unit einstein s^{-1} m^{-2}), in the Rayonet reactor was determined using the *p*-nitroanisole (PNA) / pyridine actinometer using the methods described in ref. (1), according to equation S1, where k_{PNA} (unit s^{-1}) is the measured phototransformation rate constant of PNA, Φ_{PNA} is the quantum yield of PNA phototransformation (Φ_{PNA} = 0.29×[Pyridine]+ 0.00029, unitless or mole einstein^{-1})(2), $f_{p,\lambda}$ is the normalized emission spectrum of the photoreactor lamps (unitless, see Figure S1) and $\varepsilon_{PNA,\lambda}$ is the molar absorption coefficient of PNA (unit m^2 mol^{-1}).

$$E_p^0 = \frac{k_{PNA}}{2.303\ \phi_{PNA} \sum_{\lambda = 340nm}^{410} f_{p,\lambda}\varepsilon_{PNA,\lambda}} \qquad \text{(S1)}$$

The hydroxyl radical ($^{\bullet}$OH) production rate ($r_{\bullet OH}$) and quantum yield ($\Phi_{\bullet OH}$) were determined using the conversion of benzoic acid (BA) to salicylic acid (SA). The reaction of BA with $^{\bullet}$OH yield a variety of products, including the ortho (SA), meta and para hydroxybenzoic acids. We chose to determine SA as it has a lower detection limit than the meta- or para-hydroxybenzoic acids by high performance liquid chromatography (HPLC) using fluorescence.

A stock solution (17.5mM) of BA was prepared in water and adjusted to pH 7 using concentrated (0.1M) NaOH. Dissolved organic matter (DOM) samples containing 5 mg_C L^{-1} DOC (0.42 mM) were spiked with 1 mM BA. At this BA concentration, 97.5% of the $^{\bullet}$OH produced in the system will react with the BA while the reaction of $^{\bullet}$OH with DOM will account for the remaining 2.5% (the calculation was performed using second-order rate constants $k_{BA,^{\bullet}OH}$ of 5.9×10^{9} M^{-1} s^{-1} and $k_{DOM,^{\bullet}OH}$ of 3.6×10^{8} M$_{C}^{-1}$ s^{-1}).(3, 4)

The spiked samples were irradiated for 1-2 hours in the Rayonet photoreactor and 100 µL aliquots were taken at regular time intervals. The aliquots were diluted 1:1 (v/v) with a solution of 20 mM phosphoric acid + 20mM isopropanol and the SA concentrations were measured by HPLC using the analytical method described below (Table S1).

The rate of appearance of SA, r_{SA} (unit M s^{-1}) was determined fitting a zero-order kinetics model to the SA concentration using Excel 365. The concentration of $^{\bullet}$OH was calculated from the concentration of SA produced during the irradiation corresponds divided by the yield ($Y_{BA+\bullet OH \longrightarrow SA}$) of the reaction of BA+ $^{\bullet}$OH → SA, with literature values for $Y_{BA+\bullet OH \longrightarrow SA}$ varying from 15.5% to 18% (5, 6). We chose a value of 15.5% for the calculations. The rate of production of $^{\bullet}$OH, $r_{\bullet OH}$ (unit M s^{-1}), was determined by dividing r_{SA} by $Y_{BA+\bullet OH \longrightarrow SA}$.

The $\Phi_{\bullet OH}$ can be considered to have the unit of mole einstein^{-1}. However in the present study we assume it to be unitless since we consider einstein to be equivalent to moles. $\Phi_{\bullet OH}$ is by definition the ratio of $r_{\bullet OH}$ over the rate of light absorption by DOM, r_{DOM}^{abs} (unit einstein L^{-1} s^{-1}), see equation S2:

$$\phi_{^{\bullet}OH} = \frac{r_{^{\bullet}OH}}{r_{DOM}^{abs}} \qquad \text{(S2)}$$

$\Phi_{\bullet OH}$ was determined by comparing the actinometer experiments with the BA experiments. By comparing $r_{\bullet OH}$ with the rate of PNA phototransformation (r_{PNA}, unit M s^{-1}), the extent of light absorbed in the two systems, and knowing Φ_{PNA}, one can determine $\Phi_{\bullet OH}$ using equation S3:

$$\phi_{^{\bullet}OH} = \phi_{PNA}\frac{r_{^{\bullet}OH}\sum_{\lambda=340nm}^{410} f_{p,\lambda}\varepsilon_{PNA,\lambda}}{r_{PNA}\sum_{\lambda=340nm}^{410} f_{p,\lambda}\varepsilon_{DOM,\lambda}} \qquad \text{(S3)}$$

Table S1. High Performance Liquid Chromatography analytical methods [a]

Compound	Eluent	Retention time / min	Detection wavelength (UV) or excitation / detection wavelength (fluorescence) /nm	Limit of detection [b] nM	Limit of quantification [b] nM	Standard deviation %	Measuring range
Furfuryl alcohol	65% 10mM phosphoric acid 35% Methanol	2.9	219	75	250	1	15-22.5 µM
Salicylic acid	60% 10mM phosphoric acid 40% Methanol	12	250/410	1.8	6	2	10-200 nM
p-Nitroanisole [c]	50% 10mM phosphoric acid 50% Acetonitrile	2.3	300	65	220	0.8	0.3-10 µM

[a] All the methods used were isocratic with a flow rate of 1 mL min^{-1}, the column was kept at room temperature, injection volumes 50-80 µL.

[b] Determined using the signal/noise ratio method.(7)

[c] Flow rate was 2 mL min^{-1}.

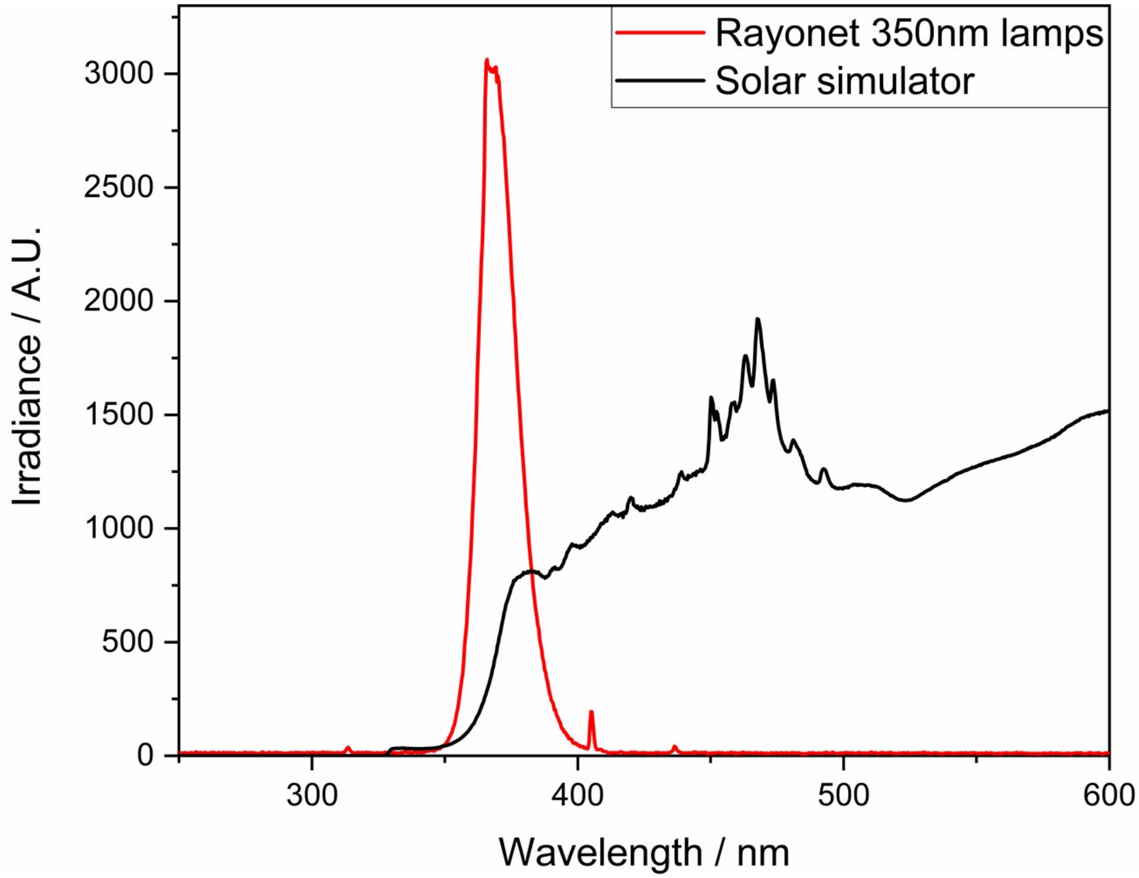

Figure S1. Photon irradiance spectra of the Rayonet reactor with RPR-3500A lamps used in the present study (red line), solar simulator from ref. (8) measured with a spectroradiometer (black line).

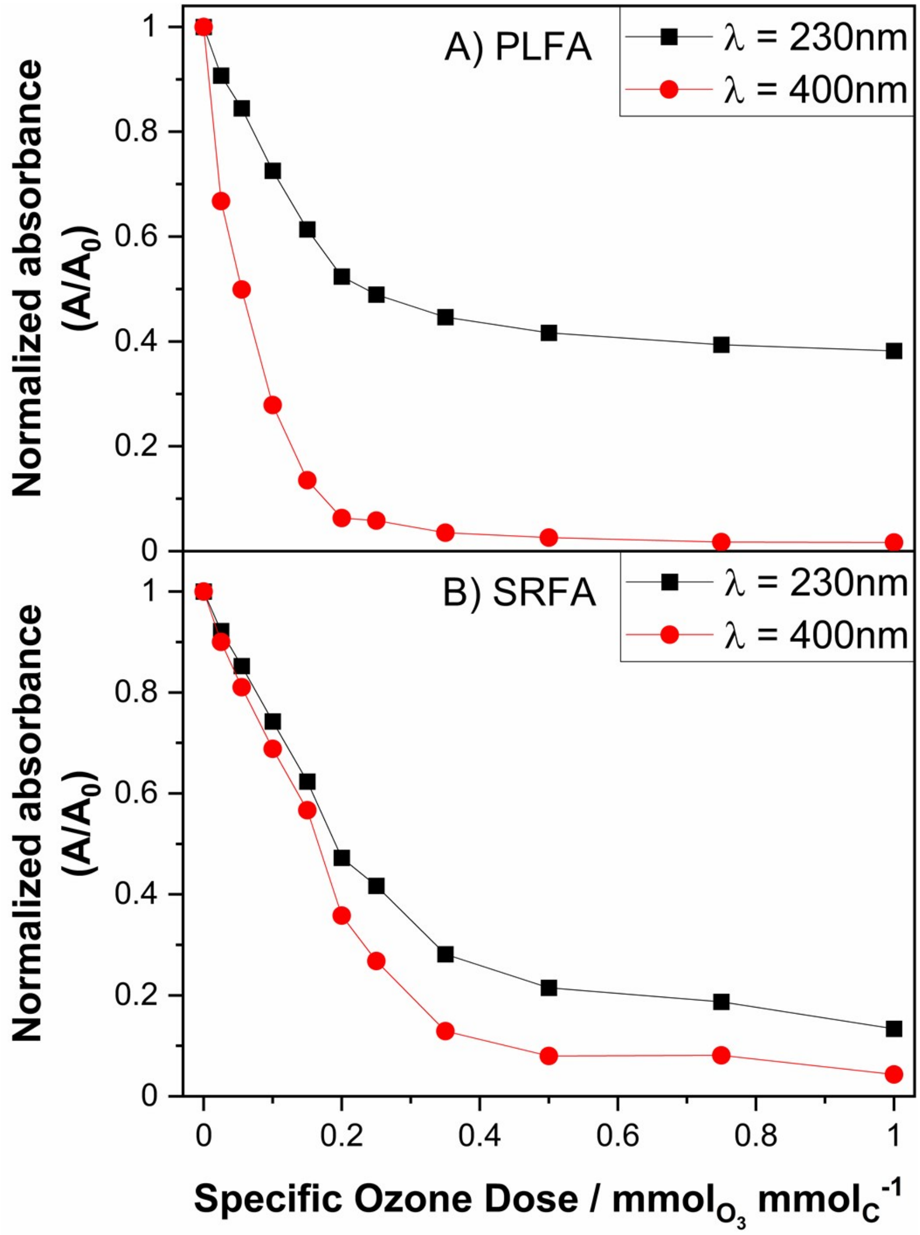

Figure S2. Effects of ozonation (specific ozone dose) on the normalized (A/A_0) light absorption for (A) Pony Lake and (B) Suwannee River fulvic acids (PLFA and SRFA, respectively). Black squares/lines: wavelength λ= 230nm. Red circles/lines: wavelength λ= 400nm. PLFA and SRFA at concentrations of 5mg$_C$ L^{-1}. Solutions were buffered with 10 mM phosphate at pH 7, with no addition of a hydroxyl radical scavenger. Lines are shown to guide the eye.

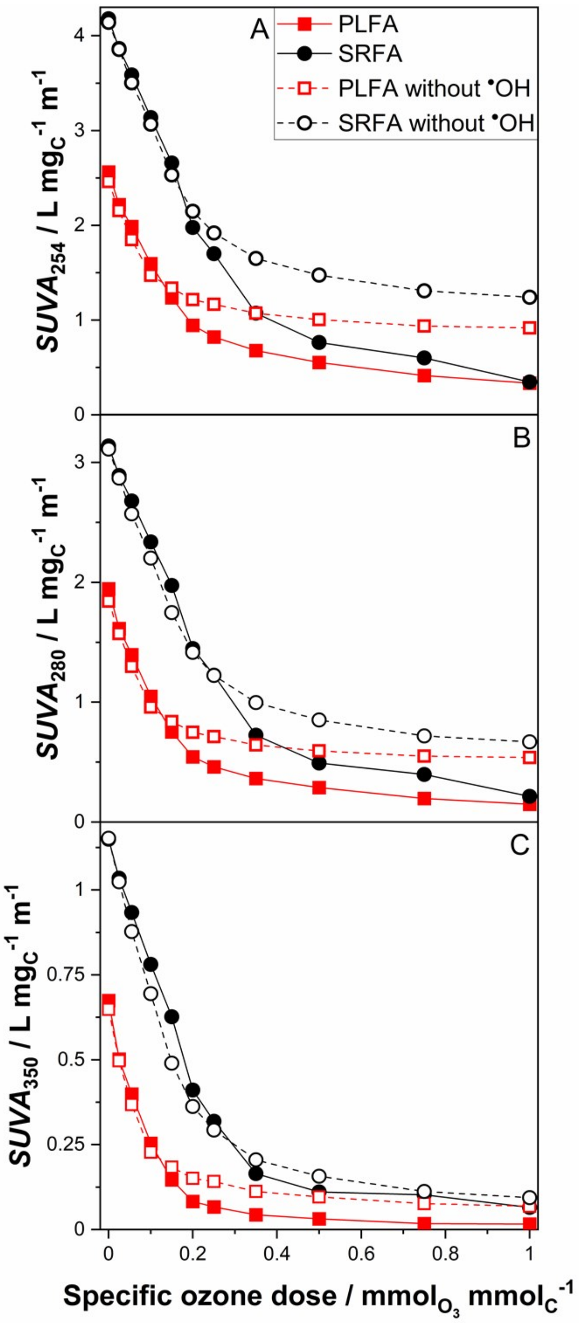

Figure S3. Specific UV-Vis absorptions at the wavelengths of λ=254, λ=280 and λ=350 ($SUVA_{254}$, $SUVA_{280}$ and $SUVA_{350}$, respectively) as a function of the specific ozone dose. Red squares/lines: PLFA; black circles/lines: SRFA. DOM at concentrations of 5mg$_C$ L^{-1}. Solutions were buffered with 10 mM phosphate at pH 7. Experiments were conducted in the absence (filled symbols) and in the presence (open symbols) of 0.1 M *t*-butanol as a hydroxyl radical scavenger. Empty symbols: data from ref. (8). Lines are shown to guide the eye.

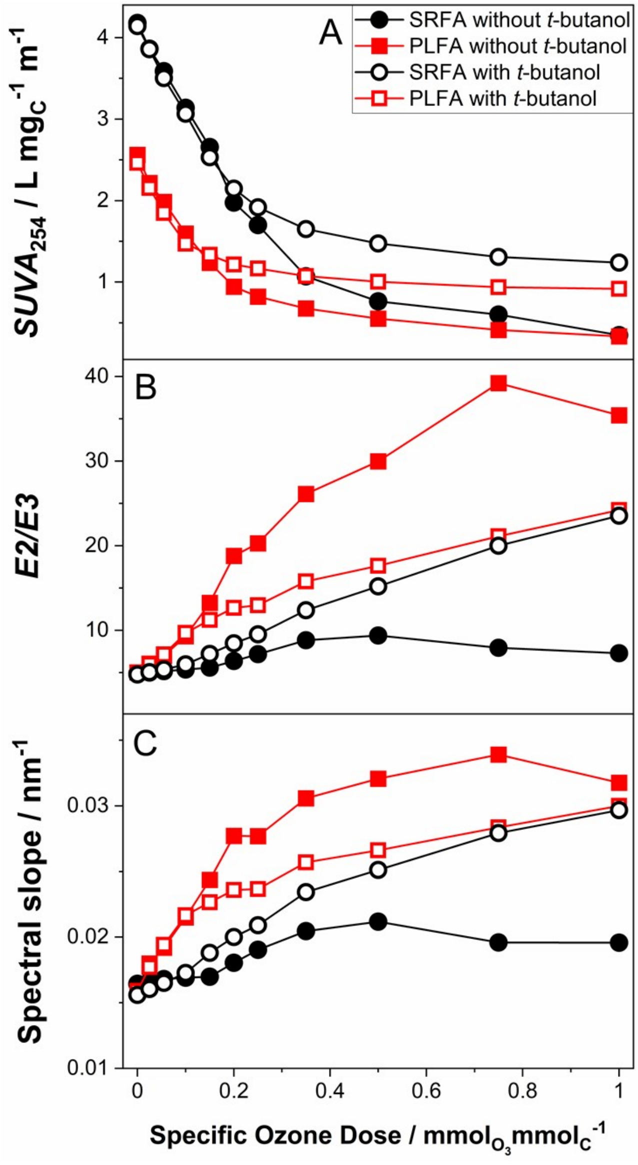

Figure S4. Evolution of several optical parameters as a function of the specific ozone dose for Pony Lake and Suwannee River fulvic acids (PLFA and SRFA, respectively). (A): Specific UV-Vis absorption at the wavelength λ=254nm (*$SUVA_{254}$*). (B): E2/E3 ratio (ratio of the Absorbance at λ=250 over the absorbance at λ=365nm). (C): Spectral slopes. Red squares/lines: PLFA; black circles/lines: SRFA. DOM at concentrations of 5mg_C L^{-1}. Solutions were buffered with 10 mM phosphate at pH 7. Empty symbols: Data from ref. (8), where the ozonation experiments were conducted in the presence of 0.1M *t*-butanol as an •OH scavenger. The lines are shown to guide the eye.

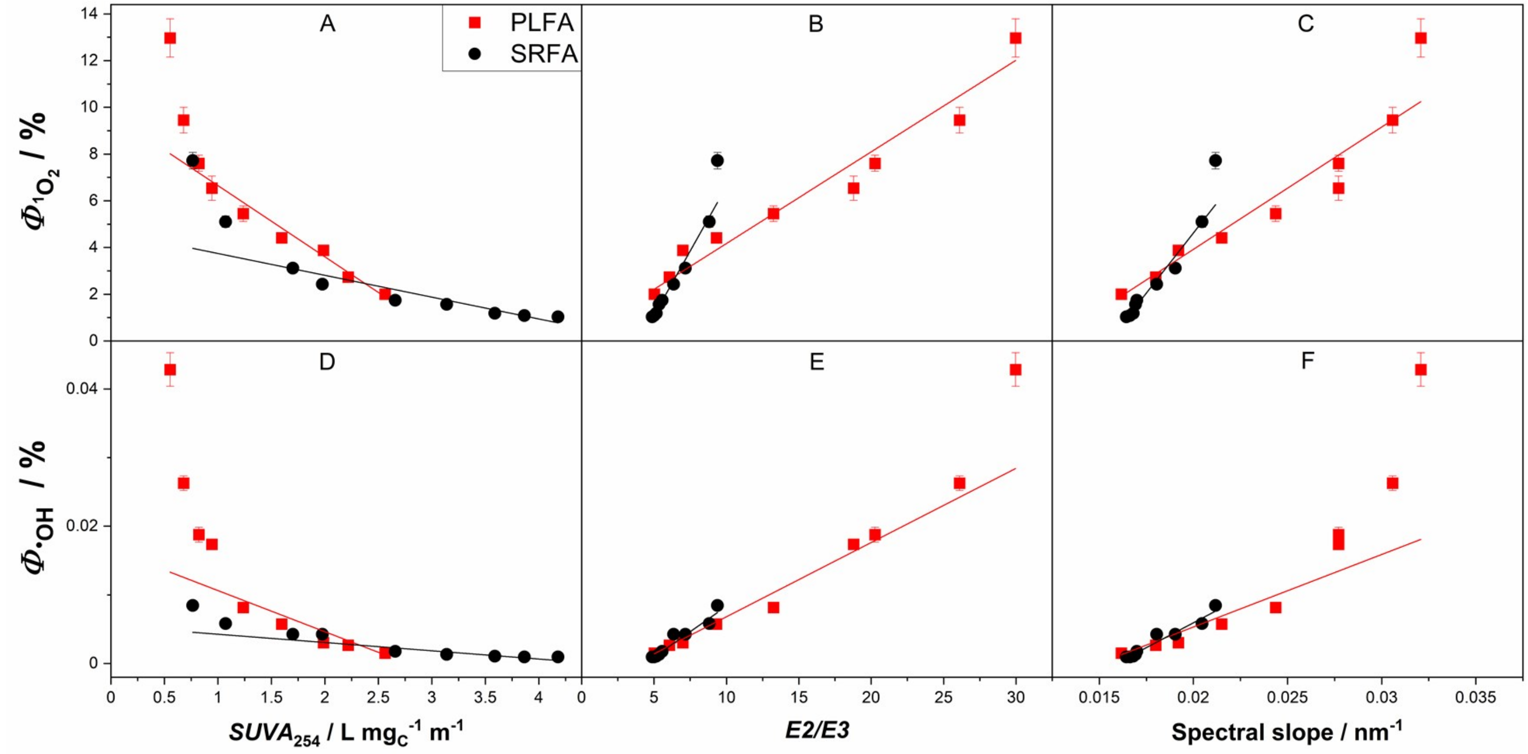

Figure S5. Relationships between several measured optical parameters and the singlet oxygen quantum yield (Φ_{1O2}) or the hydroxyl radical quantum yield ($\Phi_{\bullet OH}$) for Pony Lake and Suwannee River fulvic acids (PLFA and SRFA, respectively). (A) and (D): Φ_{1O2} and $\Phi_{\bullet OH}$ vs the specific UV absorbance at the wavelength λ=254nm ($SUVA_{254}$), respectively. (B) and (E): Φ_{1O2} and $\Phi_{\bullet OH}$ vs the E2/E3 ratio. (C) and (F): Φ_{1O2} and $\Phi_{\bullet OH}$ vs the spectral slope. Red squares/lines: PLFA; black circles/lines: SRFA. DOM at concentrations of 5mg_C L^{-1}. Solutions were buffered with 10 mM phosphate at pH 7 and no hydroxyl radical scavenger was used. Error bars represents standards errors obtained from the pseudo-first order fittings (FFA or BA experiments in duplicate). Lines are linear regression lines (see Table S2 for the regression parameters).

Table S2. Regression parameter from the linear regressions in Figure S5 and from the literature

PLFA [a]	**SRFA** [a]	**PLFA** [b]	**SRFA** [b]	**Everglade DOM** [c]
Φ_{1O2}, *E2/E3* 0.0039 ±0.0004 $R^2 = 0.94$	**Φ_{1O2}, *E2/E3*** 0.0110 ±0.0009 $R^2 = 0.95$	**Φ_{1O2}, *E2/E3*** 0.0074 ±0.0008 $R^2 = 0.90$	**Φ_{1O2}, *E2/E3*** 0.0056 ±0.0006 $R^2 = 0.91$	**Φ_{1O2}, *E2/E3*** 0.0064 $R^2 = 0.69$
$\Phi_{\bullet OH}$, *E2/E3* 0.0000108 ±0.0000008 $R^2 = 0.96$	**$\Phi_{\bullet OH}$, *E2/E3*** 0.000015 ±0.000001 $R^2 = 0.95$			**$\Phi_{\bullet OH}$, *E2/E3*** 0.0000026 $R^2 = 0.54$
Φ_{1O2}, *Spectral slope* 5.2 ±0.5 $R^2 = 0.93$	**Φ_{1O2}, *Spectral slope*** 10.3 ±1.1 $R^2 = 0.92$	**Φ_{1O2}, *Spectral slope*** 7.6 ±1.2 $R^2 = 0.82$	**Φ_{1O2}, *Spectral slope*** 6.2 ±0.5 $R^2 = 0.95$	**Φ_{1O2}, *Spectral slope*** 8.2 $R^2 = 0.8$
$\Phi_{\bullet OH}$, *Spectral slope* 0.011 ±0.002 $R^2 = 0.80$	**$\Phi_{\bullet OH}$, *Spectral slope*** 0.014 ±0.001 $R^2 = 0.95$			**$\Phi_{\bullet OH}$, *Spectral slope*** 0.0028 $R^2 = 0.37$
Φ_{1O2}, $SUVA_{254}$ -0.030 ±0.003 $R^2 = 0.92$	**Φ_{1O2}, $SUVA_{254}$** -0.009 ±0.002 $R^2 = 0.71$	**Φ_{1O2}, $SUVA_{254}$** -0.046 ±0.009 $R^2 = 0.73$	**Φ_{1O2}, $SUVA_{254}$** -0.017 ±0.002 $R^2 = 0.88$	**Φ_{1O2}, $SUVA_{254}$** -0.023 $R^2 = 0.82$
$\Phi_{\bullet OH}$, $SUVA_{254}$ -0.00006 ±0.00002 $R^2 = 0.68$	**$\Phi_{\bullet OH}$, $SUVA_{254}$** -0.000012 ±0.000003 $R^2 = 0.68$			**$\Phi_{\bullet OH}$, $SUVA_{254}$** -0.0000085 $R^2 = 0.49$

[a] Data (slope of the regression line) ± standard error obtained from the linear regression

[b] Data from Ref. (8), experiments from Ref. (8) were performed in presence of 0.1M t-butanol as a $^{\bullet}$OH quencher and Φ_{1O2} was calculated in the interval range 290-400nm.

[c] Data from Ref. (9)

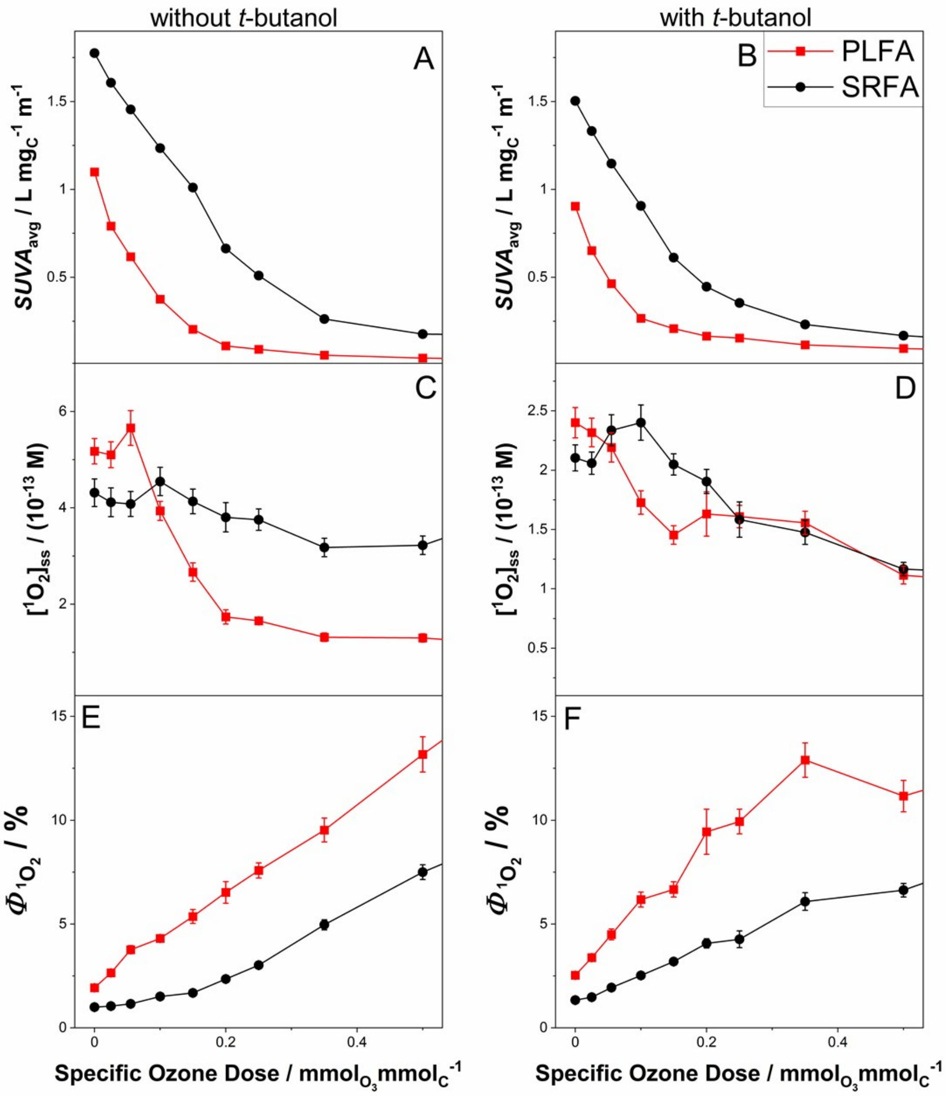

Figure S6. Effects of ozonation (specific ozone dose) on the light absorption, the generation of singlet oxygen ($^1O_2$) and the $^1O_2$ quantum yields (Φ_{1O2}) for Pony Lake and Suwannee River fulvic acids (PLFA and SRFA, respectively) in absence and presence of an $^{\bullet}$OH scavenger. (A) and (B): Specific UV-Vis absorption ($SUVA_{\mathrm{avg}}$) in the wavelengths range (A) 340-410 nm and (B) 290-400nm. (C) and (D): Measured steady-state $^1O_2$ concentration ($[^1O_2]_{ss}$) as a function of the specific ozone dose. (E) and (F): $^1O_2$ quantum yields (Φ_{1O2}). Red squares/lines: PLFA; black circles/lines: SRFA. DOM at concentrations of 5mg$_C$ L^{-1}. Solutions were buffered with 10 mM phosphate at pH 7. Error bars represent standard errors obtained from the pseudo-first order fittings (FFA experiments in duplicate). Lines are shown to guide the eye. Figures (B), (D), and (F) use data from ref. (8) for which the ozonation experiments were conducted in the presence of 0.1 M *t*-butanol as an $^{\bullet}$OH scavenger, whereas the experiments from this study (A, C, F) were performed in absence of a hydroxyl radical scavenger. Figure S6 presents the same data as Figure 2 in the main text with the addition of the data from ref. (8). Note, the irradiation setup in ref. (8) is different from this study (see Figure S1). This explains the difference in $SUVA_{\mathrm{avg}}$ for the non-ozonated sample as well as the relatively higher $[^1O_2]_{ss}$ measured here.

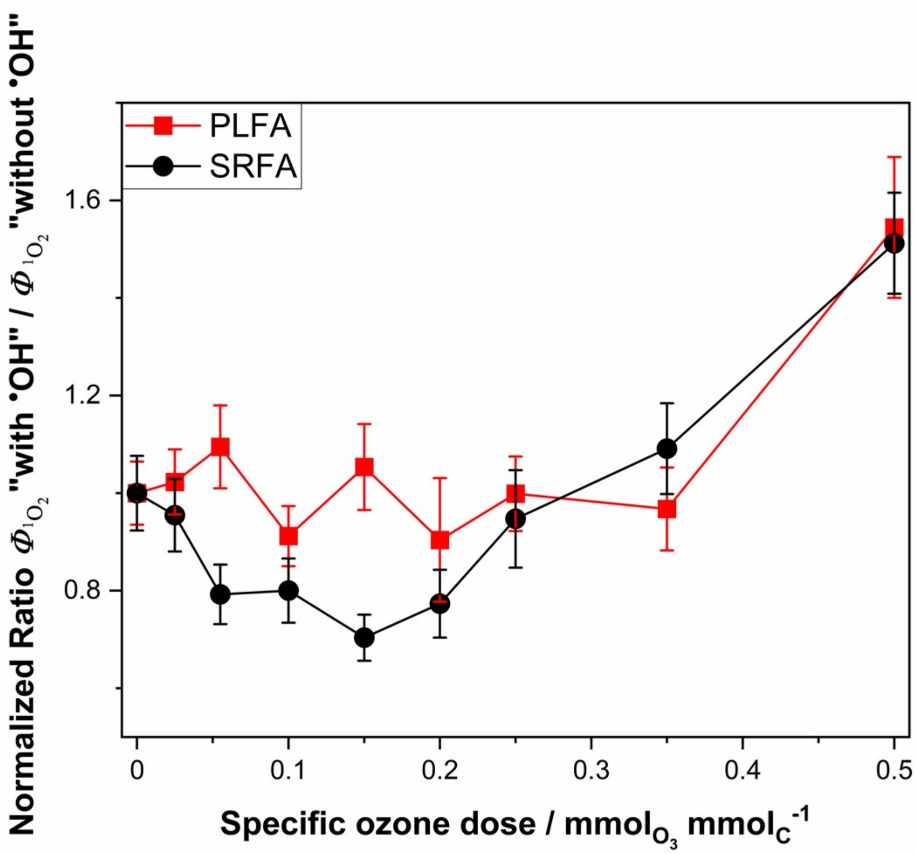

Figure S7. Normalized ratios of the singlet oxygen quantum yield (Φ_{1O2}) from this study and ref. (8). The ratios are normalized to the non-ozonated samples. The experiments in this study were performed in absence of an •OH scavenger, while those in ref. (8) were performed in presence of 0.1 M *t*-butanol as an •OH scavenger. The irradiation conditions in the current experiments were centered around 366 nm, while ref. (8) used a solar simulator (see Figure S1 for the irradiation spectra of the two setups). Φ_{1O2} were calculated in this study in the wavelength interval 340-410 nm, while for ref. (8) it was calculated in the wavelength interval 290-400nm. Red squares/lines: PLFA; black circles/lines: SRFA. DOM at concentrations of 5mg$_C$ L^{-1}. Solutions were buffered with 10 mM phosphate at pH 7. Error bars represent the propagated standard deviations (see main text). Lines are shown to guide the eye.

Table S3. Detail of the data of Figure S7. Note: the singlet oxygen quantum yield (Φ_{1O2}) is by definition the ratio of the rate of $^1O_2$ production over the rate of light absorption (quantified in Table S3 as absorbance cross section).

Specific ozone dose $mmol_{O3}$ $mmol_C^{-1}$	**Pony Lake Fulvic Acid**					
	Normalized absorbance cross section		Normalized rate of $^1O_2$ production		Ratio absorbance cross section [c]	Ratio rate of $^1O_2$ production [c]
	Ozonation "with •OH" [a]	Ozonation "without •OH" [b]	Ozonation "with •OH" [a]	Ozonation "without •OH" [b]		
0	1.00	1.00	1.00	1.00	1.00	1.00
0.025	0.72	0.72	0.99	0.97	1.00	1.02
0.055	0.56	0.51	1.09	0.91	1.10	1.20
0.1	0.34	0.30	0.76	0.72	1.16	1.06
0.15	0.19	0.23	0.52	0.61	0.81	0.85
0.2	0.10	0.18	0.34	0.68	0.54	0.49
0.25	0.08	0.17	0.32	0.67	0.47	0.48
0.35	0.05	0.13	0.25	0.65	0.41	0.39
0.5	0.04	0.10	0.25	0.46	0.35	0.54
0.75		0.08		0.42		
1		0.06		0.41		

Notes: [a] experiments from this study. [b] results from ref. (8) study. [c] ratio of the ozonation "with •OH" over the ozonation "without •OH".

Text S3. Derivation of the equation used to calculate the rate of production of SA (r_{SA}) considering its photodegradation during the experiments.

The conditions for which salicylic acid (SA) is produced by the reaction of BA with $^{\bullet}$OH and at the same time is degraded correspond to a zero-order production rate (eq. S4) followed by a first-order disappearance rate (eq. S5). The experimental data obtained are [SA] as a function of time and one has to evaluate the rate of SA disappearance separately and then calculate the production rate of SA (r_{SA}) using equation S10 that is derived in the following section.

Equations S4 and S5 and their corresponding rates of reaction can be expressed as follows, where P is a phototransformation product of SA:

$$\mathrm{BA} + h\nu \rightarrow \mathrm{SA} \qquad r_{\mathrm{SA}} = k_1 \quad \text{unit M}^{-1}\ \text{s}^{-1} \tag{S4}$$

$$\mathrm{SA} + h\nu \rightarrow \mathrm{P} \qquad r = k_2\,[\mathrm{SA}] \quad \text{unit s}^{-1} \tag{S5}$$

The differential equation for the evolution of [SA] as a function of time can be written as:

$$\frac{d\,[SA]}{dt} = k_1 - k_2\,[SA] \tag{S6}$$

Separating the variables, we obtain equation S7:

$$\frac{d\,[SA]}{k_1 - k_2\,[SA]} = dt \tag{S7}$$

This differential equation can be solved by substitution:

$\mathrm{U} = k_1 - k_2\,[\mathrm{SA}]$; $d\mathrm{U} = -k_2\,[\mathrm{SA}]$; $\mathrm{d}[\mathrm{SA}] = \mathrm{dU} / -k2$

$$\frac{d\,U}{-k_2\,U} = dt \tag{S8}$$

Equation S8 can be integrated between 0 and [SA] and 0 and t to yield equation S9:

$$\frac{\ln\,(k_1 - k_2[SA]) - \ln(k_1)}{-k_2} = t \tag{S9}$$

That can be rearranged to yield equation S10

$$[SA] = \frac{k_1\,(1 - e^{-k_2 t})}{k_2} \qquad \text{(S10)}$$

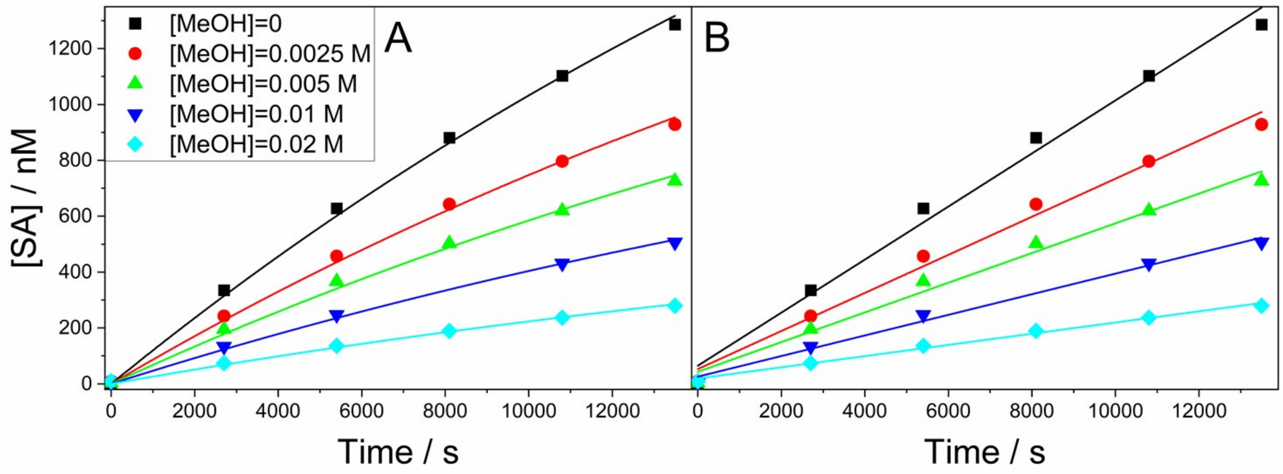

A

Model	Equation S10				
Equation	(k1*(1-exp(-k2*t)))/k2				
Plot	Methanol = 0	Methanol = 0.0025	Methanol = 0.005	Methanol = 0.01 M	Methanol = 0.02 M
k1	0.12209 ± 0.00132	0.08839 ± 0.00113	0.06917 ± 0.00106	0.04778 ± 6.28151E-4	0.02641 ± 3.81395E-4
Reduced Chi-Sqr	489.11231	357.54796	314.76927	90.23376	40.52926
R-Square (COD)	0.9979	0.99702	0.99569	0.9979	0.99607
Adj. R-Square	0.9979	0.99702	0.99569	0.9979	0.99607

B

Equation	y = a + b*x				
Plot	Methanol = 0	Methanol = 0.0025	Methanol = 0.005	Methanol = 0.01 M	Methanol = 0.02 M
Weight	No Weighting				
Intercept	65.21049 ± 40.571	53.00643 ± 29.656	43.2334 ± 25.657	25.83913 ± 15.873	19.14291 ± 6.75542
Slope	0.09496 ± 0.00496	0.06815 ± 0.00363	0.05314 ± 0.0031	0.03688 ± 0.00194	0.02004 ± 8.26385E
Residual Sum of Squar	12570.00118	6716.01892	5027.22425	1413.13654	348.49045
Pearson's r	0.99458	0.99438	0.99309	0.99588	0.99662
R-Square (COD)	0.98919	0.98879	0.98624	0.99178	0.99324
Adj. R-Square	0.98649	0.98599	0.9828	0.98904	0.99155

Figure S8. Example of fitting of an experiment set using A) equation S10. B) a zero-order kinetic linear fit. 6μM $NaNO_2$, 1mM benzoic acid, various concentration of methanol (MeOH).

Text S4. Calculation of the standard deviation

The standard deviation was calculated from the error on the HPLC probe compound measurements, the error on the UV-Vis measurements and the error of the rate constants from the literature (if available).

The standard deviation of the probe compounds (FFA or SA) and of the actinometer (PNA) measurements were calculated on each of the replicates using Origin 2018 and fitting either a first order kinetic model for FFA and PNA or a zero-order model or equation S10 for SA. Then, the errors on the mean of the two replicate experiments were calculated as the mean of the individual experimental errors.

The error of $[^1O_2]_{ss}$ ($\delta[^1O_2]_{ss}$) was calculated as $\delta[^1O_2]_{ss} = [^1O_2]_{ss} \times \sqrt{\left(\frac{\delta k_{FFA}}{k_{FFA}}\right)^2 + \left(\frac{\delta k_{FFA,1O2}}{k_{FFA,1O2}}\right)^2}$ where k_{FFA} is the measured pseudo-first order rate constant for FFA disappearance (s^{-1}), δk_{FFA} is the error on k_{FFA}, $k_{FFA,1O2} = 1.00\times10^8\ M^{-1}\ s^{-1}$ is the second-order rate constant for the reaction between $^1O_2$ and FFA(10) and $\delta k_{FFA1O2} = 4.0\times10^6\ M^{-1}\ s^{-1}$ is the error on $k_{FFA,1O2}$ from literature.(10)

$SUVA_{avg}$ was calculated using equation 7 in the main text. The error of $SUVA_{avg}$ was calculated using equation S11, where $SUVA_\lambda$ is the specific absorption coefficient at a wavelength λ (unit L $mg_C^{-1}\ m^{-1}$), A_λ is the absorbance at the wavelength λ and δA_λ is the standard error on A_λ measured from triplicate UV-Vis measurements.

$$\delta SUVA_{avg} = \sum_{\lambda = 340}^{410nm} SUVA_\lambda \sqrt{\left(\frac{\delta A_\lambda}{A_\lambda}\right)^2} \qquad \text{(S11)}$$

$\Phi_{\bullet OH}$ was calculated using equation S3. The error on $\Phi_{\bullet OH}$ was calculated using equation S12, where $r_{\bullet OH}$ and $\delta r_{\bullet OH}$ is the measured production rate of $^\bullet OH$ and its error, respectively.

$$\delta\phi_{\bullet OH} = \phi_{\bullet OH} \times \sqrt{\left(\frac{\delta r_{\bullet OH}}{r_{\bullet OH}}\right)^2 + \left(\frac{\delta k_{PNA}}{k_{PNA}}\right)^2 + \left(\frac{\delta SUVA_{avg}}{SUVA_{avg}}\right)^2} \qquad \text{(S12)}$$

The error of Φ_{1O2} was calculated using equation S13, where $k_{d,1O2,H2O} = 2.76\times10^5$ s^{-1} and $\delta k_{d,1O2,H2O} = 2\times10^3$ s^{-1} is the literature value for the deactivation of $^1O_2$ in water and its associated error, respectively.(10)

$$\delta\phi_{1_{O_2}} = \phi_{1_{O_2}} \times \sqrt{\left(\frac{\delta k_{FFA}}{k_{FFA}}\right)^2 + \left(\frac{\delta k_{PNA}}{k_{PNA}}\right)^2 + \left(\frac{\delta SUVA_{avg}}{SUVA_{avg}}\right)^2 + \left(\frac{\delta k_{d,1O2,H2O}}{k_{d,1O2,H2O}}\right)^2} \qquad \text{(S13)}$$

Origin 2018 was used in the fitting procedure to calculate the spectral slope according to equation 6 (main text) and the reported error on the spectral slope is the error on the fitting procedure.

References

1. Bahnmuller, S.; von Gunten, U.; Canonica, S., Sunlight-Induced Transformation of Sulfadiazine and Sulfamethoxazole in Surface Waters and Wastewater Effluents. *Water Res.* **2014,** *57*, 183-192.
2. Laszakovits, J. R.; Berg, S. M.; Anderson, B. G.; O'Brien, J. E.; Wammer, K. H.; Sharpless, C. M., *p*-Nitroanisole/Pyridine and *p*-Nitroacetophenone/Pyridine Actinometers Revisited: Quantum Yield in Comparison to Ferrioxalate. *Environ. Sci. Technol. Lett.* **2017,** *4* (1), 11-14.
3. Buxton, G. V.; Greenstock, C. L.; Helman, W. P.; Ross, A. B., Critical-Review of Rate Constants for Reactions of Hydrated Electrons, Hydrogen-Atoms and Hydroxyl Radicals ($^{\bullet}$OH/$^{\bullet}$O-) in Aqueous-Solution. *J. Phys. Chem. Ref. Data* **1988,** *17* (2), 513-886.
4. Westerhoff, P.; Aiken, G.; Amy, G.; Debroux, J., Relationships Between the Structure of Natural Organic Matter and its Reactivity Towards Molecular Ozone and Hydroxyl Radicals. *Water Res.* **1999,** *33* (10), 2265-2276.
5. Qian, J. G.; Mopper, K.; Kieber, D. J., Photochemical Production of the Hydroxyl Radical in Antarctic Waters. *Deep Sea Res. Oceanogr. Res. Pap.* **2001,** *48* (3), 741-759.
6. Anastasio, C.; McGregor, K. G., Chemistry of Fog Waters in California's Central Valley: 1. In Situ Photoformation of Hydroxyl Radical and Singlet Molecular Oxygen. *Atmos. Environ.* **2001,** *35* (6), 1079-1089.
7. VICH guideline GL2, Validation of analytical procedures: methodology. London: European Medicines Agency, 1998.
8. Leresche, F.; McKay, G.; Kurtz, T.; von Gunten, U.; Canonica, S.; Rosario-Ortiz, F. L., Effects of Ozone on the Photochemical and Photophysical Properties of Dissolved Organic Matter. *Environ. Sci. Technol.* **2019,** *53* (10), 5622-5632.
9. McKay, G.; Huang, W. X.; Romera-Castillo, C.; Crouch, J. E.; Rosario-Ortiz, F. L.; Jaffe, R., Predicting Reactive Intermediate Quantum Yields from Dissolved Organic Matter Photolysis Using Optical Properties and Antioxidant Capacity. *Environ. Sci. Technol.* **2017,** *51* (10), 5404-5413.
10. Appiani, E.; Ossola, R.; Latch, D. E.; Erickson, P. R.; McNeill, K., Aqueous Singlet Oxygen Reaction Kinetics of Furfuryl Alcohol: Effect of Temperature, pH, and Salt Content. *Environ. Sci.-Process Impacts* **2017,** *19* (4), 507-516.